Mechanisms for the Proton Mobility-Dependent Gas-Phase Fragmentation Reactions of S-alkyl Cysteine Sulfoxide-Containing Peptide Ions

Jennifer M. Froelich[a] and Gavin E. Reid[a,b]

[a] Department of Chemistry, Michigan State University, East Lansing, Michigan, USA
[b] Department of Biochemistry and Molecular Biology, Michigan State University, East Lansing, Michigan, USA

Mechanisms for the gas-phase fragmentation reactions of singly and multiply protonated precursor ions of the model S-alkyl cysteine sulfoxide-containing peptides GAILCGAILK, GAILCGAILR, and VTMGHFCNFGK prepared by reaction with iodomethane, iodoacetamide, iodoacetic acid, acrylamide, or 4-vinylpyridine, followed by oxidation with hydrogen peroxide, as well as peptides obtained from an S-carboxyamidomethylated and oxidized tryptic digest of bovine serum albumin, have been examined using multistage tandem mass spectrometry, hydrogen/deuterium exchange and molecular orbital calculations (at the B3LYP/6-31 + G(d,p) level of theory). Consistent with previous reports, CID-MS/MS of the S-alkyl cysteine sulfoxide-containing peptide ions resulted in the dominant "non-sequence" neutral loss of an alkyl sulfenic acid (XSOH) from the modified cysteine side chains under conditions of low proton mobility, irrespective of the alkylating reagent employed. Dissociation of uniformly deuterated precursor ions of these model peptides determined that the loss of alkyl sulfenic acid in each case occurred via a "charge-remote" five-centered *cis*-1,2 elimination reaction to yield a dehydroalanine-containing product ion. Similarly, the charge state dependence to the mechanisms and product ion structures for the losses of CO_2, CO_2 + H_2O and CO_2 + CH_2O from S-carboxymethyl cysteine sulfoxide-containing peptides, and for the losses of $CH_2CHCONH_2$ and $CH_2CHC_5H_4N$, respectively, from S-amidoethyl and S-pyridylethyl cysteine sulfoxide-containing peptide ions have also been determined. The results from these studies indicate that both the proton mobility of the peptide precursor ion and the nature of the S-alkyl substituent have a significant influence on the abundances and charge states of the product ions resulting from the various competing fragmentation pathways. (J Am Soc Mass Spectrom 2007, 18, 1690–1705) © 2007 American Society for Mass Spectrometry

Conventional approaches for mass spectrometry based protein identification and characterization typically involve the reduction and alkylation of cysteine residues before enzymatic digestion [1–4]. Numerous reports in the literature have demonstrated that the resulting thio-ether bonds are susceptible to oxidation, either during the enzymatic digestion process or subsequent sample handling steps, before mass spectrometry analysis [5–8]. These reports have also demonstrated that fragmentation of the resultant S-alkyl cysteine sulfoxide-containing peptides under low-energy collision induced dissociation (CID)-tandem mass spectrometry (MS/MS) conditions can result in the formation of abundant product ions via cleavages occurring within the modified cysteine side chains [5–8]. While these "non-sequence" ions are indicative of the presence of the modified amino acid residue within the peptide, their formation at high abundance may "suppress" the formation of desired "sequence" ion information, thereby limiting the utility of "de novo" analysis strategies [9] or current database search algorithms [10, 11] employed for the identification and characterization of these modified peptide ions. Thus, it is important to determine the conditions, such as charge state and peptide composition (i.e., proton mobility), under which these non-sequence fragmentation pathways are observed as dominant processes. Furthermore, given that MS^3 dissociation of abundant non-sequence product ions may often be employed to obtain additional sequence information to facilitate further structural characterization [12, 13], it is also important to determine the mechanisms responsible for their formation, and the structures of the resultant product ions.

Anecdotal evidence from the literature suggests that the loss of XSOH from S-alkyl cysteine sulfoxide-containing peptides (Scheme **1**, pathway A) occurs as a dominant fragmentation process primarily from singly protonated peptide ions [5, 6]. Consistent with these observations, the mechanism responsible for the loss of

Address reprint requests to Dr. G. E. Reid, Department of Chemistry, Michigan State University, 234 Chemistry Building, East Lansing, Michigan 48824, USA. E-mail: reid@chemistry.msu.edu

1044-0305/07/$32.00
doi:10.1016/j.jasms.2007.06.014

Published online July 11, 2007
Received May 10, 2007
Revised June 28, 2007
Accepted June 28, 2007

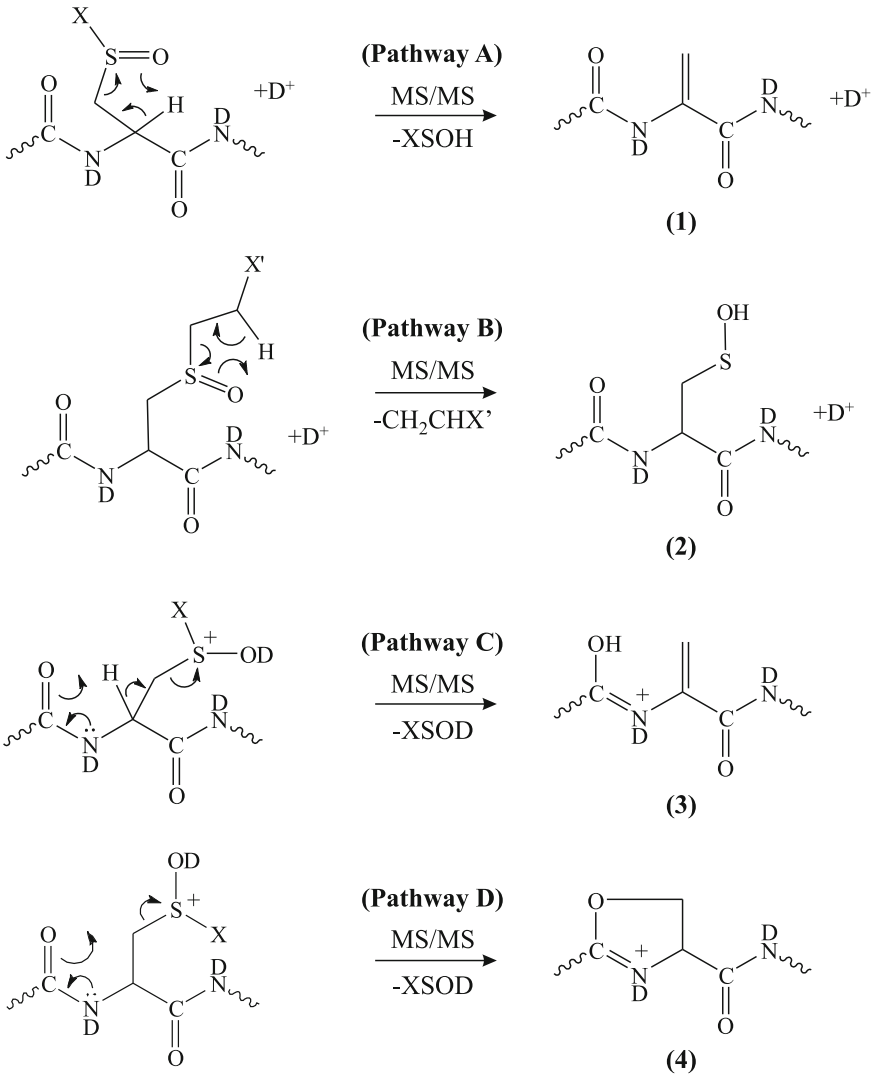

Scheme 1. Potential mechanisms for the loss of XSOH or CH_2CHX' from the side chains of S-alkyl cysteine sulfoxide-containing peptide ions.

XSOH from S-alkyl cysteine sulfoxide-containing peptides formed by reaction with iodoacetamide, where X = CH_2CONH_2, has been proposed to occur via a "charge-remote" *cis*-1,2 elimination reaction involving transfer of the α-hydrogen atom to yield an acyclic dehydroalanine-containing product ion **(1)** (Scheme **1**, pathway A) [6, 7]. A similar *cis*-1,2 elimination mechanism, yielding a cysteine sulfenic acid-containing product ion **(2)** (Scheme **1**, pathway B), has also been proposed for the loss of CH_2CHX' from S-alkyl cysteine sulfoxide-containing peptides formed by reaction with acrylamide (X′ = $CONH_2$) [5] or vinylpyridine (X′ = C_5H_4N) [8], as well as for the loss of $C_6H_7NO_2$ from S-alkyl cysteine sulfoxide-containing peptides formed by reaction with N-ethylmaleimide [8]. These mechanistic proposals are also consistent with those previously determined for the fragmentation of methionine sulfoxide-containing peptide ions, where the dominant side-chain loss of CH_3SOH occurs via a charge-remote *cis*-1,2 elimination reaction under conditions of low proton mobility [14, 15]. Note however, that alternative "charge-directed" mechanisms for the loss of XSOH from S-alkyl cysteine sulfoxide-containing peptides should also be considered, involving the formation of a protonated dehydroalanine product ion **(3)** (Scheme **1**, pathway C) via an E2 elimination reaction (this ion would have the same primary structure, but different site of protonation to the dehydroalanine product ion formed via pathway A), or the formation of a five-membered protonated oxazoline product ion **(4)** via an S_N2 neighboring group participation reaction (Scheme **1**, pathway D).

To date, however, detailed experimental studies to determine the mechanisms and the proton mobility dependence to these fragmentation reactions, as well as to determine the mechanisms responsible for the subsequent fragmentation reactions of the initial product ions, have not been carried out. Here, by using a combination of multistage tandem mass spectrometry (MS/MS, MS^3, and MS^4), hydrogen/deuterium ex-

change reactions and molecular orbital calculations (at the B3LYP/6-31 + G(d,p) level of theory), we have obtained experimental evidence for the proton mobility dependence and mechanisms responsible for the loss of XSOH and CH_2CHX' from singly and multiply protonated S-alkyl cysteine sulfoxide-containing peptide ions prepared by reaction with the commonly employed alkylating reagents iodomethane, iodoacetamide, iodoacetic acid, acrylamide and 4-vinylpyridine.

Experimental

Materials

Unless stated otherwise, all reagents were analytical reagent (AR) grade and used as supplied without further purification. The synthetic model "tryptic" peptides GAILCGAILK (CK), VTMGHFCNFGK (MCK), GAILMGAILK (MK), and GAILMGAILR (MR) were purchased from GenScript (Piscataway, NJ). GAILCGAILR (CR) was obtained from New England Peptide, Inc. (Gardner, MA). Acrylamide (electrophoresis grade) and dithiothreitol (DTT) were from Boehringer Mannheim Corporation (Indianapolis, IN). Iodomethane, iodoacetamide, iodoacetic acid, 4-vinylpyridine, guanidine hydrochloride, Trizma base, Trizma hydrochloride, methanol (HPLC grade), monodeuterated acetic acid (CH_3CO_2D), and bovine serum albumin were purchased from Sigma (St. Louis, MO). Deuterium oxide (D_2O) and deuterated methanol (CD_3OD) were obtained from Cambridge Isotope Laboratories (Andover, MA). Hydrogen peroxide (30% aqueous solution) was from Columbus Chemical Industries (Columbus, WI). Glacial acetic acid (ACS grade) and formic acid (ACS grade) were purchased from Spectrum Chemicals (Gardena, CA). Acetonitrile (HPLC grade) was obtained from EMD Chemicals (Gibbstown, NJ). Sequencing grade modified trypsin was from Promega (Madison, WI). All solutions were prepared using deionized water purified by a Barnstead nanopure diamond purification system (Dubuque, IA).

S-alkylation of Cysteine-Containing Peptides

Cysteine-containing peptides (1 mg) were individually dissolved in 1 mL of 500 mM Tris (pH 7.8) containing 25 mM alkylating reagent and reacted at room temperature for 20 min (iodoacetamide), 30 min (iodomethane and iodoacetic acid), 60 min (acrylamide), or 120 min (4-vinylpyridine). The samples were then immediately de-salted (Sep-Pak Classic C_{18}; Waters, Milford, MA) and dried completely by centrifugal evaporation.

Oxidation of S-Alkyl Cysteine- and Methionine-Containing Peptides

S-alkyl cysteine- and methionine-containing peptides were resuspended in 30% hydrogen peroxide-containing 5% acetic acid and allowed to react at room temperature for 30 min. The samples were then immediately de-salted before their introduction into the mass spectrometer.

Mass Spectrometry of Model Peptides

Peptides (0.04 mg/mL) dissolved in 50% methanol, 1% acetic acid were introduced to a linear quadrupole ion trap mass spectrometer (Thermo model LTQ; San Jose, CA) by nanospray ionization (nanoESI) at 0.5 μL/min. The spray voltage was maintained at 1.8 kV. The heated capillary temperature was 200°C. Uniformly labeled hydrogen/deuterium exchanged peptides were prepared by repeatedly drying and dissolving the sample (0.4 mg/mL) in 50% CD_3OD/50% D_2O containing 0.17 M CH_3CO_2D. Then, samples were diluted and introduced to a quadrupole ion trap mass spectrometer (Thermo model LCQ Deca) by electrospray ionization (ESI) at 4 μL/min. Typical ESI conditions were: spray voltage, 5 kV; nitrogen sheath gas, 25 psi; heated capillary temperature, 200°C. Nitrogen auxiliary gas (15, arbitrary units) was added to minimize deuterium back exchange during electrospray sample introduction. CID-MS/MS and MS^n experiments on both the LTQ and LCQ instruments were performed on monoisotopically mass selected ions using standard isolation and excitation procedures. The spectra shown are the average of 80 scans.

Preparation of Oxidized Tryptic Protein Digests

Bovine serum albumin (200 μg) was dissolved in 100 μL of 6 M guanidine/500 mM Tris (pH 7.8) and 10 mM DTT, then heated at 37°C for 1 h. Iodoacetamide was then added to a final concentration of 21 mM followed by incubation for 20 min at room temperature. The solution was then diluted with 380 μL of water and sequencing grade modified trypsin was added at an enzyme: substrate ratio of 1:20 (wt/wt). Protein digestion was performed overnight at 37°C after which the sample was immediately desalted by Sep-Pak Classic C_{18} solid-phase extraction. Then, before LC-MS/MS analysis, oxidation of both methionine and S-carboxyamidomethyl cysteine residues within the resultant peptide mixture was carried out by reaction in 30% hydrogen peroxide-containing 5% acetic acid for 30 min at room temperature.

Liquid Chromatography/Mass Spectrometry of Oxidized Protein Digests

LC-MS/MS was performed using a Paradigm MS4 capillary RP-HPLC system (Michrom Bioresources, Auburn, CA) directly coupled to a linear quadrupole ion trap mass spectrometer (Thermo model LTQ) equipped with nanospray ionization (nanoESI). RP-HPLC conditions were as follows: 75 μm i.d. × 150 mm fused silica column packed with Magic C18 (5 μm, 200 Å) operated at a flow rate of 0.25 μL/min using a linear 80 min gradient from 5% to 45% Solvent B. Solvent A was

0.05% formic acid in H_2O and Solvent B was 0.05% formic acid in CH_3CN. The spray voltage was maintained at 1.8 kV. The heated capillary temperature was 200°C. Three pmol of the oxidized digest prepared in 97.9% H_2O/2% CH_3CN/0.1% formic acid were injected to obtain product ion spectra with high quality signal-to-noise ratios for subsequent peptide identification and quantitative analysis of product ion abundances. The mass spectrometer was operated in a data-dependent mode where the five most abundant precursor ions identified above a preset threshold of 1.0×10^4 counts following the acquisition of a full MS scan (*m/z* 300–1700) were isolated and subjected to CID-MS/MS. Dynamic exclusion was enabled with a repeat count of three and an exclusion duration set to 90 s.

MS/MS Database Analysis

Uninterpreted MS/MS spectra were searched against the sequence of bovine serum albumin using the SEQUEST algorithm (Thermo Finnigan) [10] with the following parameters: Enzyme type: trypsin; number of possible missed cleavage sites: 3; precursor mass tolerance: 1.5; peptide mass tolerance: 2.0. All spectra were searched with dynamic mass modifications of +16.0 u (methionine sulfoxide), +57.0 u (S-carboxyamidomethyl cysteine), and +73.0 u (S-carboxyamidomethyl cysteine sulfoxide). Manual inspection of each spectrum was performed to validate all SEQUEST identifications.

Quantitative Analysis of Product Ion Abundances

Quantitative evaluation of non-sequence product ion abundances in the model S-alkyl cysteine sulfoxide- or methionine sulfoxide-containing peptide ions were performed by cleavage intensity ratio (CIR) calculations, essentially as described previously [14,15]. Product ion abundances were first normalized by dividing the experimentally observed abundances by the square root of their charge states. Then, CIR calculations were performed by dividing the normalized abundance of the non-sequence product ion by the average normalized abundance of all the product ions observed from all cleavage sites within the peptide. CIR values greater than 1.0 are indicative of an "enhanced" cleavage, while values less than 1.0 indicate a "suppressed" cleavage. The fractional abundance of product ions formed by sequential fragmentations (i.e., formation of a non-sequence product ion followed by further loss of H_2O or by further sequence ion fragmentation, or vice versa) included in the non-sequence CIR calculations were based on the relative abundances of the individual non-sequence and sequence product ions from which they were formed.

Quantitative analysis of non-sequence product ions from the oxidized tryptic digest of bovine serum albumin were performed by first filtering the spectra to remove any ions present below 50 counts (empirically determined to be a reasonable approximation of the level of chemical noise in the spectra). Then, the percent total product ion abundances were obtained by expressing the summed abundances of product ions formed by the loss of H_2NCOCH_2SOH, as well as the fractional abundance of product ions resulting from sequential losses (i.e., formation of a non-sequence product ion followed by immediate sequence ion fragmentation, or vice versa), as a fraction of the total product ion abundance.

Molecular Orbital Calculations

Low-energy transition-state structures were initially located at the PM3 semi-empirical level of theory, then subjected to further optimization at the B3LYP/6-31 + G(d,p) level of theory using the GAUSSIAN 98 molecular modeling package [16]. Intrinsic reaction coordinate (IRC) searches were then performed, followed by geometry optimizations to locate the appropriate reactant and product ion structures associated with each transition state. All optimized structures were subjected to harmonic vibrational frequency analysis and visualized using the computer package GaussView 2.1 to determine the nature of the stationary points. Zero point energies were obtained from harmonic frequency calculations without scaling. Complete structural details and lists of vibrational frequencies for each structure are available from the authors.

Results and Discussion

Multistage Tandem Mass Spectrometry and H/D Exchange Reactions for the Fragmentation of S-Methyl and S-Carboxyamidomethyl Cysteine Sulfoxide-Containing Peptide Ions

The product ion spectra obtained by CID-MS/MS of the singly and doubly protonated precursor ions of the cysteine sulfoxide-containing peptide GAILCGAILK [C(S-me)(ox)K], (where me = CH_3), prepared by reaction with iodomethane followed by oxidation with hydrogen peroxide, are shown in Figure 1a and b, respectively. In both cases, product ions corresponding to the neutral loss of CH_3SOH (64Da) from the S-alkyl cysteine sulfoxide side chain were observed as the most abundant fragmentation processes. Differentiation of the charge-remote versus charge-directed mechanisms proposed in Scheme **1** for the loss of CH_3SOH from these ions was readily achieved by CID-MS/MS of their uniformly deuterated precursor ions. Fragmentation via the charge-remote *cis*-1,2 elimination reaction (Scheme **1**, pathway A) would result in the loss of CH_3SOH, while fragmentation via the charge-directed pathways (Scheme **1**, pathways C and D) would result in the loss of CH_3SOD. The insets to Figure 1a and b show expanded regions of the product ion spectra obtained by CID-MS/MS of the uniformly deuterated $[M + D]^+$ and $[M + 2D]^{2+}$ precursor ions of C(S-me)(ox)K. The loss of CH_3SOH (64Da) was observed for both precur-

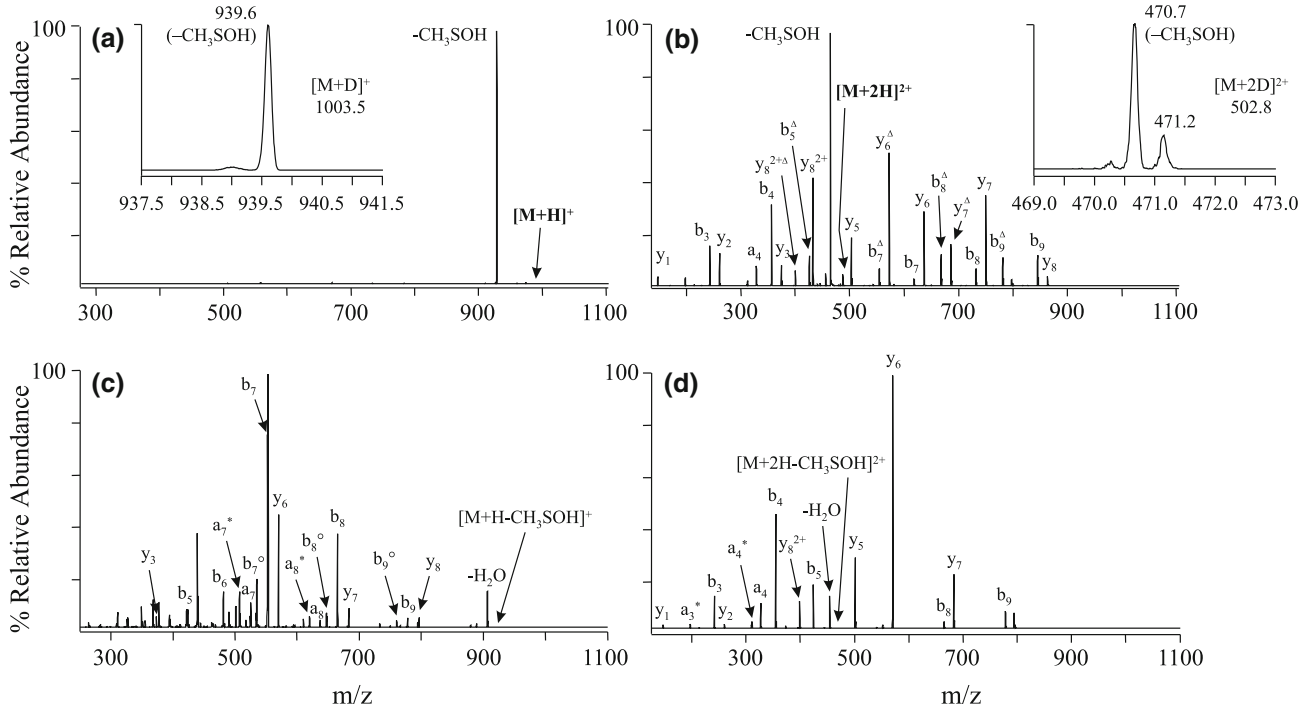

Figure 1. Multistage tandem mass spectrometry of the S-methyl cysteine sulfoxide-containing peptide GAILCGAILK [C(S-me)(ox)K]. (**a**) CID-MS/MS product ion spectrum of the $[M + H]^+$ ion. (**b**) CID-MS/MS product ion spectrum of the $[M + 2H]^{2+}$ ion. (**c**) CID MS^3 product ion spectrum of the $[M + H - CH_3SOH]^+$ neutral loss product ion from (**a**). (**d**) CID MS^3 product ion spectrum of the $[M + 2 - CH_3SOH]^{2+}$ neutral loss product ion from (**b**). The insets to **a** and **b**, showing expanded regions of the product ion spectra obtained by CID-MS/MS of the uniformly deuterated $[M + D]^+$ and $[M + 2D]^{2+}$ precursor ions, confirm that the loss of CH_3SOH occurs via the charge-remote *cis*-1,2 elimination pathway. Key: open triangle: $-CH_3SOH$; open circle: $-H_2O$.

sor ions, confirming that fragmentation had occurred via the charge-remote *cis*-1,2 elimination mechanism.

Given that the neutral loss of CH_3SOH was observed as the exclusive fragmentation process following MS/MS of the singly protonated precursor ion (Figure 1a), and as the most abundant fragmentation process following MS/MS of the doubly protonated precursor ion (Figure 1b), MS^3 dissociation of the $[M + H - CH_3SOH]^+$ and $[M + 2H - CH_3SOH]^{2+}$ product ions from these spectra was employed to obtain additional sequence ions for further structural characterization and to further confirm the mechanism responsible for the neutral losses (Figure 1c and d, respectively). The b_5 and y_6 ions observed in the MS^3 product ion spectrum of the $[M + H - CH_3SOH]^+$ ion, and the b_4, b_5, y_5, and y_6 product ions observed in the MS^3 product ion spectrum of the $[M + 2H - CH_3SOH]^{2+}$ ion, all corresponding to fragmentation on either side of the dehydroalanine-containing product, provided further evidence for the *cis*-1,2 elimination mechanism. Notably, it can also be seen by comparison of Figure 1b and d, that MS^3 of the $[M + 2H - CH_3SOH]^{2+}$ ion resulted in a product ion spectrum with equivalent sequence information, but reduced spectral complexity compared with that obtained by MS/MS of the $[M + 2H]^{2+}$ ion, where abundant product ions corresponding to sequential fragmentations of both non-sequence side chain and sequence peptide backbone cleavage sites were observed.

The proton mobility dependence to the abundances of the non-sequence side-chain cleavage product ions from the singly and doubly protonated C(S-me)(ox)K precursor ions, as well as from the singly and doubly protonated precursor ions of the S-methyl cysteine sulfoxide-containing peptide GAILCGAILR [C(S-me)(ox)R] and the singly, doubly, and triply protonated precursor ions of the methionine sulfoxide- and S-methyl cysteine sulfoxide-containing peptide VTMGHFCNFGK [M(ox)C(S-me)(ox)K], was quantitatively evaluated by cleavage intensity ratio (CIR) calculations performed on each of the non-sequence product ions [14,15] (Table 1). These data clearly indicate that loss of the side chain is a more dominant process under "non-mobile" and "partially mobile" proton conditions, i.e., where the number of ionizing protons is ≤ the combined number of basic residues (Arg, Lys, or His), compared with that observed under "mobile" proton conditions, where the number of ionizing protons is > the combined number of basic residues (Arg, Lys, or His) [15].

For the methionine sulfoxide- and S-methyl cysteine sulfoxide-containing peptide M(ox)C(S-me)(ox)K, the neutral loss of CH_3SOH could result from side-chain cleavage of the S-methyl cysteine sulfoxide or methionine sulfoxide residues, or both. However, given the

Table 1. Cleavage intensity ratio (CIR) values for the "non-sequence" side chain fragmentation reactions of S-alkyl cysteine sulfoxide- and methionine sulfoxide-containing peptide ions

Peptide	X=	Precursor ion charge state	Calculated CIR value			
			−XSOH[d]	−(X-H)[d]	$-CO_2$[d]	$-CH_3SOH$ from Met(ox)
GAILC(X)(ox)GAILK (C(X)(ox)K)	CH_3	+1[b]	11.0	0	—	—
		+2[c]	3.9	0	—	—
	CH_2CONH_2	+1[b]	10.8	0	—	—
		+2[c]	2.5	0	—	—
	CH_2CO_2H	+1[b]	6.5	0	5.4	—
		+2[c]	2.4	0	0	—
	$CH_2CH_2CONH_2$	+1[b]	5.4	6.6	—	—
		+2[c]	3.9	2.6	—	—
	$CH_2CH_2C_5H_4N$	+1[b]	10.0	2.0	—	—
		+2[c]	0	12.0[f]	—	—
		+3[c]	0	10.9[f]	—	—
GAILC(X)(ox)GAILR (C(X)(ox)R)	CH_3	+1[a]	11.0	0	—	—
		+2[c]	4.0	0	—	—
	CH_2CONH_2	+1[a]	10.9	0	—	—
		+2[c]	3.1	0	—	—
	CH_2CO_2H	+1[a]	5.3	0	6.6	—
		+2[c]	3.5	0	0	—
	$CH_2CH_2CONH_2$	+1[a]	4.9	6.9	—	—
		+2[c]	4.0	2.2	—	—
	$CH_2CH_2C_5H_4N$	+1[a]	10.8	1.2	—	—
		+2[c]	0	12.0[f]	—	—
		+3[c]	0	11.7[f]	—	—
VTM(ox)GHFC(X)(ox)NFGK (M(ox)C(X)(ox)K)	CH_3	+1[b]	12.9[e]	0	—	—
		+2[b]	12.6[e]	0	—	—
		+3[c]	5.7[e]	0	—	—
	CH_2CONH_2	+1[b]	12.2	0	—	0.2
		+2[b]	12.2	0	—	0.1
		+3[c]	5.1	0	—	0.1
	CH_2CO_2H	+1[b]	7.0	0	6.9	0
		+2[b]	9.0	0	4.7	0
		+3[c]	4.0	0	6.3	0
	$CH_2CH_2CONH_2$	+1[b]	7.3	6.5	—	0.1
		+2[b]	9.3	4.6	—	0
		+3[c]	3.7	8.0	—	0
	$CH_2CH_2C_5H_4N$	+1[b]	11.2	2.5	—	0.1
		+2[b]	1.5	12.5[g]	—	0
		+3[c]	0	14.0[f]	—	0
GAILM(ox)GAILK (M(ox)K)		+1[b]	—	—	—	9.3
		+2[c]	—	—	—	0.1
GAILM(ox)GAILR (M(ox)R)		+1[a]	—	—	—	10.9
		+2[c]	—	—	—	0.2

[a]"Non-mobile" proton [14, 15].
[b]"Partially" mobile proton [14, 15].
[c]"Mobile" proton [14, 15].
[d]Contributions from sequential losses are included in the CIR calculation.
[e]Corresponds to side chain cleavage from Cys(X)(ox) and/or Met(ox).
[f]Observed exclusively as a charged loss.
[g]Observed as both charged and neutral losses.

minimal loss of CH_3SOH observed during MS/MS of the methionine sulfoxide- and S-carboxyamidomethyl cysteine sulfoxide-containing peptide M(ox)C(S-cam)(ox)K (where cam = CH_2CONH_2), and the similar fragmentation behaviors of the S-methyl and S-carboxyamidomethyl cysteine sulfoxide-containing peptides C(S-me)(ox)K and C(S-cam)(ox)K (see below), it is expected that loss from the S-methyl cysteine sulfoxide residue was the dominant process.

Essentially identical spectra to those discussed above for dissociation of the S-methyl cysteine sulfoxide-containing peptide ions were also obtained following CID-MS/MS of the singly, doubly, or triply protonated precursor ions of the S-carboxyamidomethyl cysteine sulfoxide-containing peptides C(S-cam)(ox)K, C(S-cam)(ox)R and M(ox)C(S-cam)(ox)K formed by reaction with iodoacetamide and oxidation with hydrogen peroxide (Table 1). Hydrogen/deuterium exchange fol-

lowed by MS/MS, as well as MS^3 of the resultant $[M + nH - H_2NCOCH_2SOH]^{nH+}$ product ions, confirmed that the side-chain neutral loss of H_2NCOCH_2SOH (107Da) from these peptides also occurred exclusively via the charge-remote *cis*-1,2 elimination reaction mechanism shown in pathway A of Scheme **1**. As expected, the spectra obtained by MS^3 dissociation of the $[M + nH - H_2NCOCH_2SOH]^{nH+}$ product ions were identical to those from the S-methyl cysteine sulfoxide-containing peptides (data not shown).

Notably, the CIR values calculated for the losses of CH_3SOH or H_2NCOCH_2SOH from the doubly protonated (i.e., mobile proton) S-methyl and S-carboxyamidomethyl cysteine sulfoxide-containing derivatives of GAILCGAILK (CIR values of 3.9 and 2.5, respectively) and GAILCGAILR (CIR values of 4.0 and 3.1, respectively), were significantly higher than the CIR values calculated for the loss of CH_3SOH from the doubly protonated precursor ions of the equivalent methionine sulfoxide-containing peptides GAILM(ox)GAILK (CIR 0.1) and GAILM(ox)GAILR (CIR 0.2)°(Table°1).°Furthermore,°while°the°mechanism°for the side-chain fragmentation from the doubly protonated methionine sulfoxide derivative was previously demonstrated to occur via a charge-directed mechanism

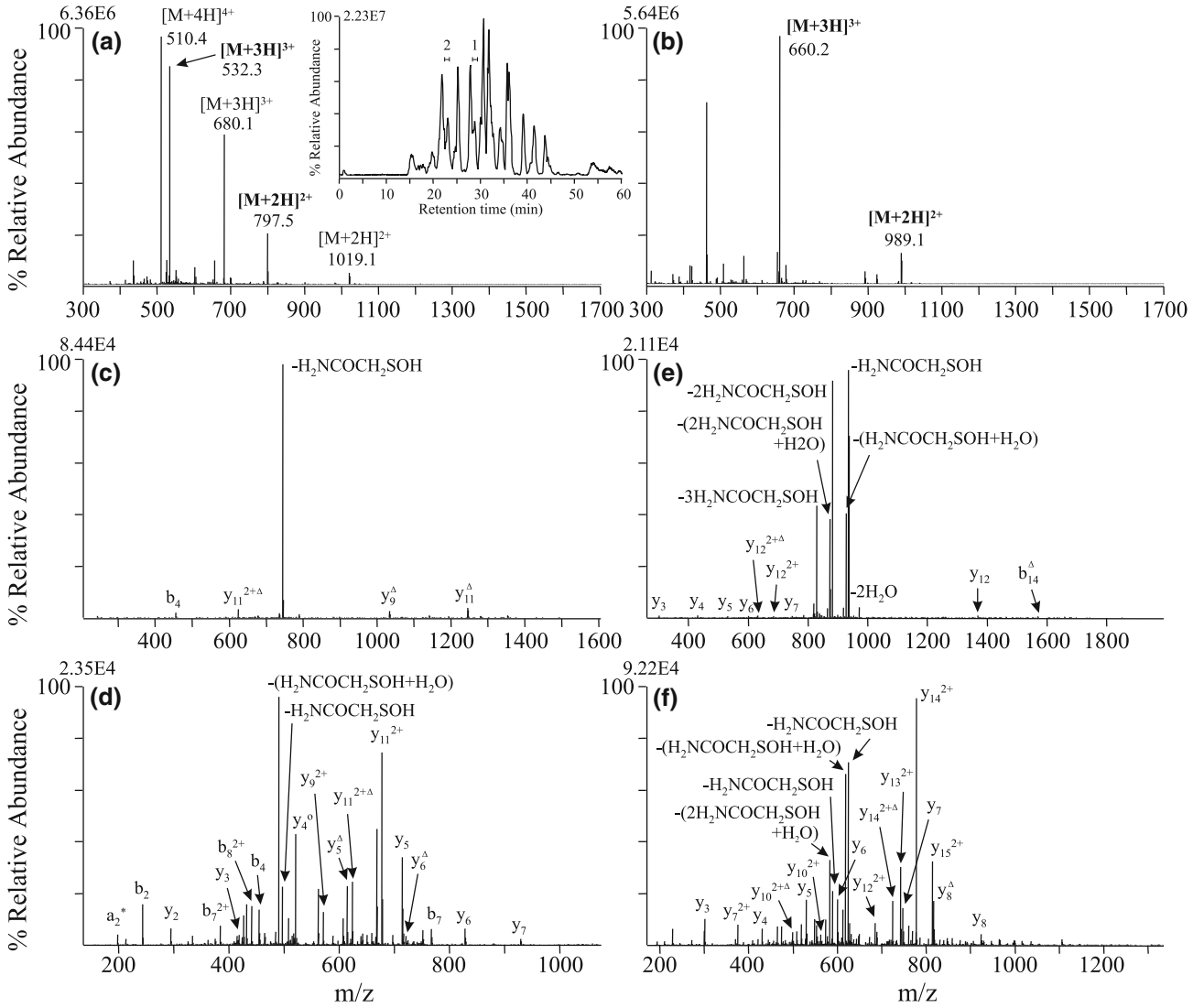

Figure 2. Capillary HPLC-mass spectrometry analysis of S-carboxyamidomethyl cysteine sulfoxide [S-cam(ox)] containing peptides from an oxidized tryptic digest of bovine serum albumin. Mass spectra obtained from region 1 (28.2–29.2 min) and region 2 (22.5–23.5 min) of the LC-MS chromatogram [shown in the inset to (**a**)] are shown in (**a**) and (**b**), respectively. The CID-MS/MS product ion spectra obtained from dissociation of the doubly (*m/z* 797.5) and triply (*m/z* 532.3) protonated precursor ions of the singly oxidized peptide LKPDPNTLC[S-cam(ox)]DEFK in (**a**) are shown in (**c**) and (**d**), respectively. The CID-MS/MS product ion spectra obtained from dissociation of the doubly (*m/z* 989.1) and triply (*m/z* 660.2) protonated precursor ions of the triply oxidized peptide C[S-cam(ox)]C[S-cam(ox)]AADDKEAC[S-cam(ox)]FAVEGPK in (**b**) are shown in (**e**) and (**f**), respectively. Key: open triangle: $-H_2NCOCH_2SOH$; open circle = $-H_2O$.

Table 2. Percent total product ion abundances for the "non-sequence" side chain neutral loss of H_2NCOCH_2SOH from S-carboxyamidomethyl (S-cam) cysteine sulfoxide-containing peptide ions of an oxidized tryptic digest of bovine serum albumin

	% Total product ion abundance[a]				
	Precursor ion charge state				
Peptide sequence	+1	+2	+3	+4	+5
GAC(S-cam(ox))LLPK	57.5[d]	14.5[e]	—	—	—
SLHTLFGDELC(S-cam(ox))K	73.7[d]	49.9[d]	22.4[e]	—	—
YIC(S-cam(ox))DNQDTISSK	—	44.9[e]	—	—	—
C(S-cam(ox))C(S-cam)TESLVNR[b]	—	48.3[e]	—	—	—
EYEATLEEC(S-cam(ox))C(S-cam(ox))AK	—	29.3[e]	—	—	—
DDPHAC(S-cam(ox))YSTVFDK	—	51.9[d]	25.9[e]	—	—
RPC(S-cam(ox))FSALTPDETYVPK	—	81.3[d]	21.8[e]	—	—
LFTFHADIC(S-cam(ox))TLPDTEK	—	55.8[d]	30.9[e]	—	—
M(ox)PC(S-cam(ox))TEDYLSLILNR	—	30.5[e]	0.5[e]	—	—
LAKEYEATLEEC(S-cam(ox))C(S-cam(ox))AK	—	84.1[d]	44.9[e]	—	—
C(S-cam(ox))C(S-cam)AADDKEAC(S-cam(ox))FAVEGPK[c]	—	86.2[d]	21.7[e]	—	—
C(S-cam(ox))C(S-cam(ox))AADDKEAC(S-cam(ox))FAVEGPK	—	89.4[d]	15.1[e]	—	—
VASLRETYGDM(ox)ADC(S-cam(ox))C(S-cam(ox))EK	—	—	53.2[e]	—	—
YNGVFQEC(S-cam(ox))C(S-cam(ox))QAEDK	—	69.1[d]	20.9[e]	—	—
YNGVFQEC(S-cam(ox))C(S-cam(ox))QAEDKGAC(S-cam(ox))LLPK	—	—	75.1[e]	—	—
LKEC(S-cam(ox))C(S-cam(ox))DKPLLEK	—	—	92.8[d]	74.0[d]	—
VHKEC(S-cam(ox))C(S-cam(ox))HGDLLEC(S-cam(ox))ADDR	—	—	87.8[d]	36.1[d]	—
LKPDPNTLC(S-cam(ox))DEFK	—	82.4[d]	20.5[e]	—	—
LKPDPNTLC(S-cam(ox))DEFKADEK	—	76.0[d]	61.7[d]	9.7[e]	—
NEC(S-cam(ox))FLSHKDDSPDLPK	—	76.0[d]	59.6[d]	23.9[e]	—
QEPERNEC(S-cam(ox))FLSHKDDSPDLPK	—	—	80.3[d]	60.3[d]	34.0[e]

[a]Contributions from sequential losses are included in the calculation.
[b]Site of oxidation could be at either of the cysteine residues.
[c]Site of oxidation could be at either of the two N-terminal cysteine residues.
[d]"Partially" mobile proton [14, 15].
[e]"Mobile" proton [14, 15].

[14], the side-chain losses from the S-alkyl cysteine sulfoxide-containing peptides were observed to occur via the charge-remote mechanism. These observations can be rationalized as being due to the increased acidity of the α-hydrogen atom of the S-alkyl cysteine sulfoxide side chain compared with the β-hydrogen atoms of the methionine sulfoxide side chain.

Further examples of the proton mobility dependence to the preferential side-chain fragmentation behavior of S-carboxyamidomethyl cysteine sulfoxide residues are shown in Figure 2 and in Table 2. Figure 2a and b show selected mass spectra obtained by capillary HPLC-mass spectrometry analysis of an S-carboxyamidomethylated and oxidized tryptic digest of bovine serum albumin, prepared by reduction and alkylation with iodoacetamide, followed by oxidation with hydrogen peroxide. The CID-MS/MS product ion spectra obtained by dissociation of the doubly (*m/z* 797.5) and triply (*m/z* 532.3) protonated precursor ions in Figure 2a are shown in Figure 2c and d, respectively. SEQUEST analysis of these spectra, followed by manual verification of the search results, enabled the peptide to be identified as the singly oxidized LKPDPNTLC[S-cam(ox)]DEFK. It can be seen that the non-sequence loss of H_2NCOCH_2SOH dominated the product ion spectrum (82.4% total product ion abundance) for the doubly protonated precursor ion (i.e., partially mobile proton conditions). In contrast, the same loss (including the sequential loss of H_2O) was only observed at 20.5% total product ion abundance from dissociation of the triply protonated precursor ion (i.e., mobile proton conditions), with numerous abundant sequence product ions also being observed. The remaining doubly, triply, and quadruply protonated ions in Figure 2a were found to correspond to the singly oxidized peptide LKPDPNTLC[S-cam(ox)]DEFKADEK (Table 2).

Interestingly, dissociation of the doubly protonated precursor ion at *m/z* 989.1 in Figure 2b resulted in the sequential loss of up to three H_2NCOCH_2SOH neutral molecules, with a combined total product ion abundance of 89.4% (see Figure 2e). This peptide was subsequently identified by SEQUEST analysis and manual verification of the search results as the triply oxidized peptide C[S-cam(ox)]C[S-cam(ox)]AADDKEAC[S-cam(ox)]FAVEGPK. Similar to that seen in Figure 2d, however, dissociation of this peptide (Figure 2f) under mobile proton conditions (i.e., the triply protonated precursor ion at *m/z* 660.2 in Figure 2b) resulted in substantially less abundant non-sequence ions (combined total product ion abundance of 15.1%) and the formation of extensive sequence information.

These data, as well as those obtained from the oxidized peptides in Table 2, indicate that the formation

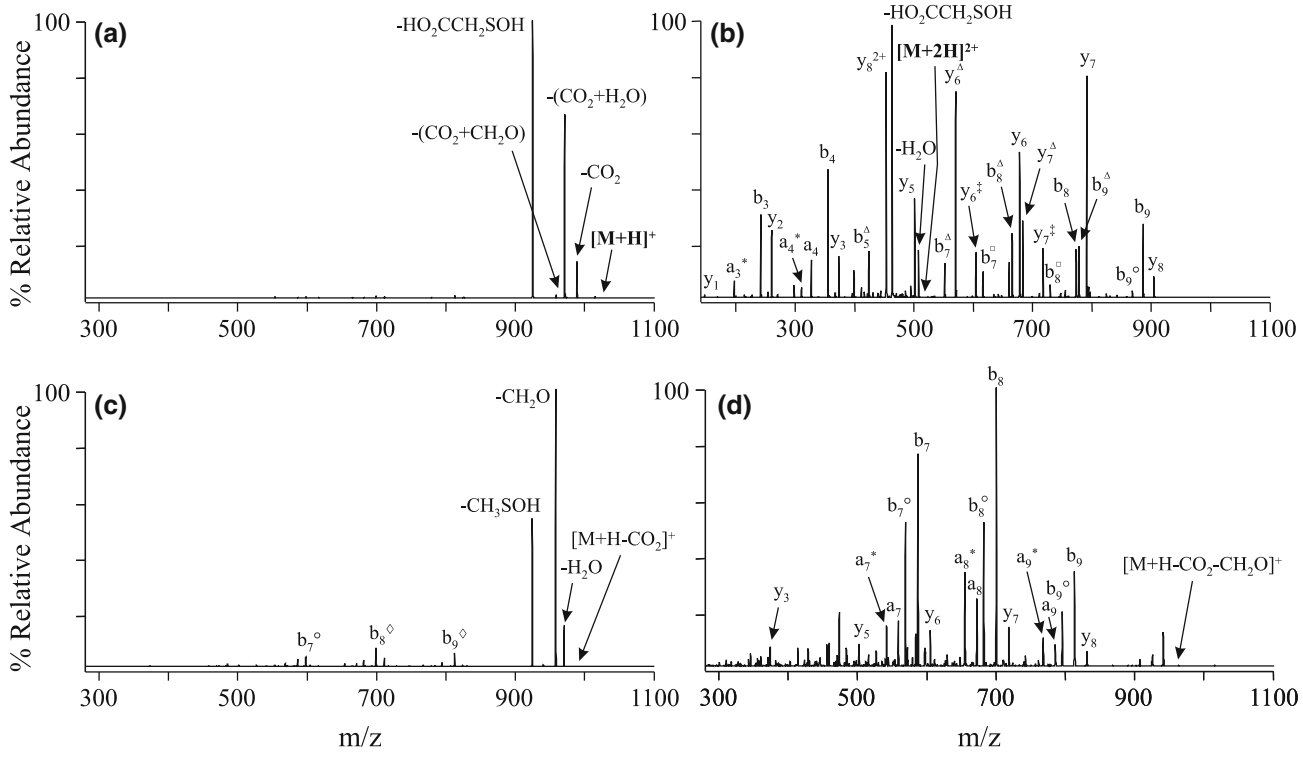

Figure 3. Multistage tandem mass spectrometry of the S-carboxymethyl cysteine sulfoxide-containing peptide GAILCGAILK [C(S-cm)(ox)K]. (**a**) CID-MS/MS product ion spectrum of the $[M + H]^+$ ion. (**b**) CID-MS/MS product ion spectrum of the $[M + 2H]^{2+}$ ion. (**c**) CID MS^3 product ion spectrum of the $[M + H - CO_2]^+$ neutral loss product ion from (**a**). (**d**) CID MS^4 product ion spectrum of the $[M + H - CH_2O]^+$ neutral loss product ion from (**c**). Key: open triangle: $-HO_2CCH_2SOH$; open square: $-CO_2$; double dagger: $-(CO_2+CH_2O)$; open diamond: $-CH_2O$; open circle = $-H_2O$.

of abundant product ions corresponding to the loss of H_2NCOCH_2SOH under conditions of low proton mobility allows both the presence and number of S-carboxyamidomethyl cysteine sulfoxide residues within a given peptide to be readily determined. This information can be particularly useful to assist in identification of the peptide when sequence ions are present at low abundance. For example, automated SEQUEST analysis of the spectra obtained by CID-MS/MS of the triply protonated precursor ion of the peptide LKEC[S-cam(ox)]C[S-cam(ox)]DKPLLEK (Table 2) resulted in this peptide being included as only the second ranked candidate. However, manual interrogation of the spectrum enabled the observation of product ions corresponding to the loss of up to two H_2NCOCH_2SOH neutral molecules with a combined total product ion abundance of 92.8%, indicating that the peptide contained two S-carboxyamidomethyl cysteine sulfoxide residues. Given that the higher ranked candidate sequence corresponded to a peptide with only one oxidized cysteine residue, it could be immediately discounted, thereby bringing the correct sequence to the top of the candidate list. This is an approach that is directly analogous to those recently described for identification of phosphoserine- or phosphothreonine-containing peptide product ion spectra that give rise to the dominant loss of H_3PO_4 upon CID-MS/MS [17, 18].

Multistage Tandem Mass Spectrometry and H/D Exchange Reactions for the Fragmentation of S-Carboxymethyl Cysteine Sulfoxide-Containing Peptide Ions

Similar to that previously reported by Steen et al. [6], CID-MS/MS of the singly and multiply protonated precursor ions of the S-carboxymethyl cysteine sulfoxide-containing peptides GAILCGAILK [C(S-cm)(ox)K] (where cm = CH_2CO_2H), GAILCGAILR [C(S-cm)(ox)R] and VTMGHFCNFGK [M(ox)C(S-cm)(ox)K], formed by reaction with iodoacetic acid and hydrogen peroxide, resulted in the side-chain neutral loss of carboxymethyl sulfenic acid (HO_2CCH_2SOH, 108Da). Figure 3a and b show the product ion spectra obtained following CID-MS/MS of the singly and doubly protonated precursor ions of C(S-cm)(ox)K. The CIR values calculated for these ions, as well as those for the C(S-cm)(ox)R and M(ox)C(S-cm)(ox)K peptides are given in Table 1. Hydrogen/deuterium exchange experiments performed on the singly and doubly protonated precursor ions of the C(S-cm)(ox)K peptide confirmed that the side-chain neutral loss of HO_2CCH_2SOH occurred via the charge-remote *cis*-1,2 elimination reaction mechanism shown in pathway A of Scheme **2**. Furthermore, MS^3 dissociation of the $[M + nH - HO_2CCH_2SOH]^{nH+}$ product ions

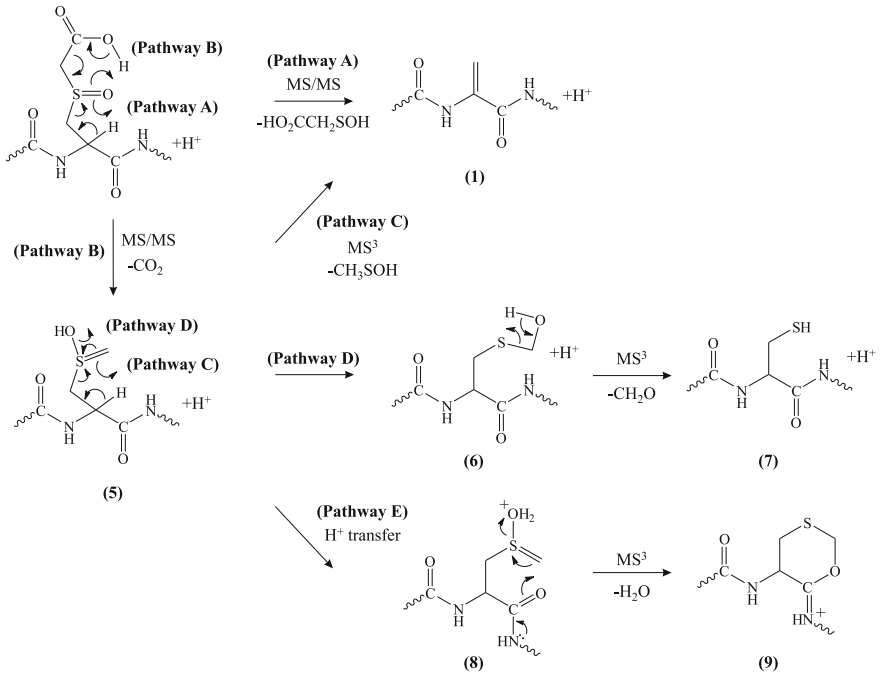

Scheme 2. Proposed mechanisms for the side-chain fragmentation reactions of S-carboxymethyl (S-cm) cysteine sulfoxide-containing peptide ions.

were identical to those from the S-methyl cysteine sulfoxide-containing peptides (data not shown).

In addition to the loss of HO_2CCH_2SOH, losses of CO_2 (44Da), CO_2+H_2O (62Da), and CO_2+CH_2O (74Da) were also observed following CID-MS/MS of the singly protonated precursor ion of C(S-cm)(ox)K (Figure 3a). A dissociation pathway that would account for the neutral loss of CO_2 is shown in pathway B of Scheme **2**, resulting in the formation of the enol form of S-methyl cysteine sulfoxide **(5)**. MS^3 dissociation of the $[M + H - CO_2]^+$ neutral loss product ion from Figure 3a resulted in the dominant side-chain neutral losses of CH_3SOH, CH_2O and H_2O (Figure 3c). The neutral loss of CH_3SOH likely occurs via a charge-remote *cis*-1,2 elimination reaction (pathway C of Scheme **2**) to yield the acyclic dehydroalanine product ion **(1)**. MS^4 of the $[M + H - CO_2 - CH_3SOH]^+$ ion resulted in an identical product ion spectrum to that shown in Figure 1c, thereby providing evidence for the proposed mechanism (data not shown). Rearrangement of the $[M + H - CO_2]^+$ product ion via a hydroxymethylthio-containing intermediate **(6)** (pathway D of Scheme **2**) would readily enable the neutral loss of CH_2O to yield the cysteine-containing product ion **(7)**. Experimental evidence for this mechanism was obtained by comparison of the MS^4 product ion spectrum obtained by dissociation of the $[M + H - CO_2 - CH_2O]^+$ product ion (Figure 3d) against the CID-MS/MS product ion spectrum of the singly protonated precursor ion of the peptide GAILCGAILK (CK) (data not shown). The spectra were essentially identical with regard to the observed b- and y-type product ion abundances, clearly indicating that the cysteine side chain had been formed. The neutral loss of H_2O from the $[M + H - CO_2]^+$ product ion likely occurs via intramolecular proton transfer from the peptide to the hydroxyl group of **(5)** to yield **(8)** (pathway E of Scheme **2**), followed by nucleophilic attack from either the carbonyl group of the C-terminal amide bond to yield the cyclic six-membered 1,3-oxathiane product ion **(9)** or the carbonyl oxygen of the N-terminal amide bond to yield a cyclic seven-membered 1,3,6-oxathiazepine product ion (structure not shown). Support for the proposed H^+ transfer mechanism was provided by observation of the loss of D_2O from the uniformly deuterated $[M + D - CO_2]^+$ product ion (data not shown).

Multistage Tandem Mass Spectrometry, H/D Exchange Reactions, and Molecular Orbital Calculations for the Fragmentation of S-Amidoethyl and S-Pyridylethyl Cysteine Sulfoxide-Containing Peptide Ions

Consistent with a previous report by Swiderek et al. [5], CID-MS/MS of protonated precursor ions of S-amidoethyl cysteine sulfoxide-containing peptides, formed by reaction with acrylamide and hydrogen peroxide, resulted in dominant side-chain neutral losses of carboxyamidoethyl sulfenic acid ($H_2NCOCH_2CH_2SOH$, 121Da), acrylamide ($CH_2CHCONH_2$, 71Da), and $CH_2CHCONH_2+H_2O$ (89Da). Figure 4a and b show the product ion spectra obtained from dissociation of the singly and doubly protonated precursor ions of the S-amidoethyl cysteine sulfoxide-containing peptide GAILCGAILK [C(S-ae)(ox)K] (where ae =

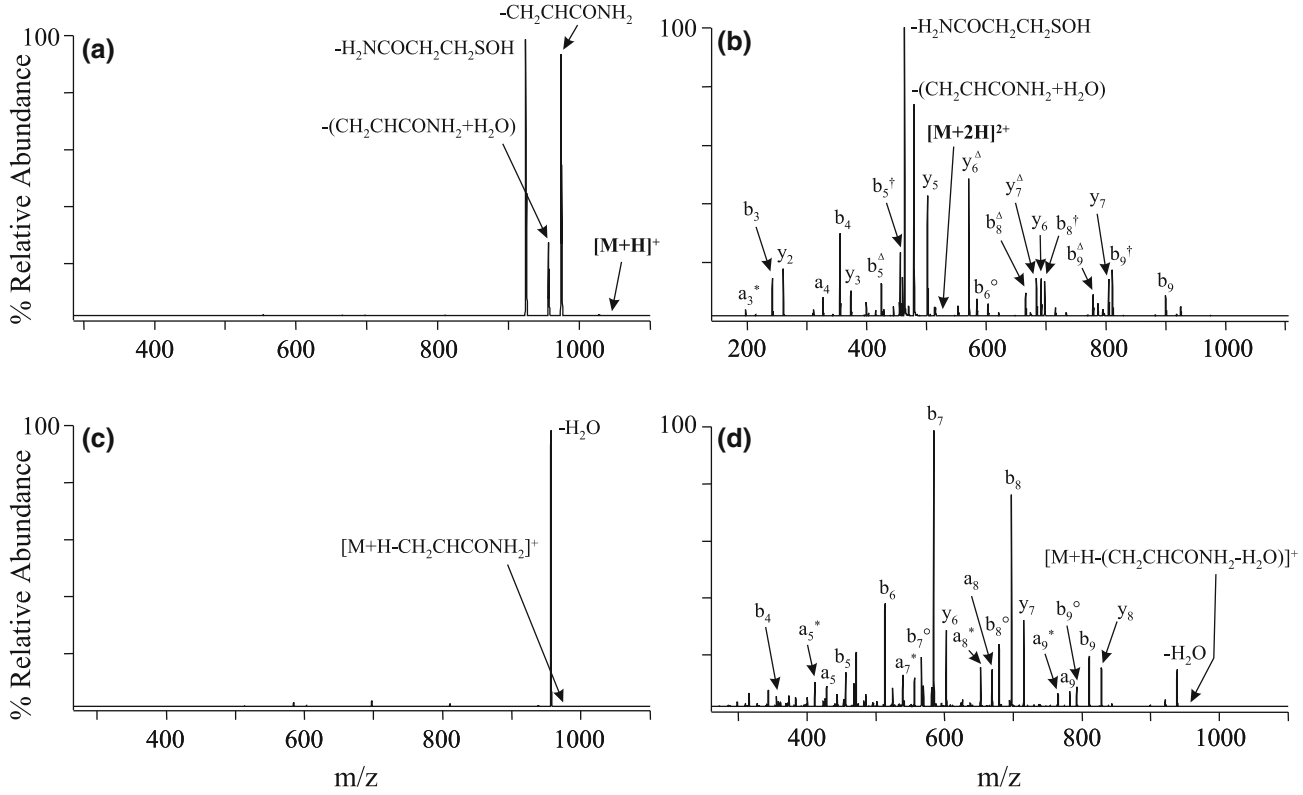

Figure 4. Multistage tandem mass spectrometry of the S-amidoethyl cysteine sulfoxide-containing peptide GAILCGAILK [C(S-ae)(ox)K]. (**a**) CID-MS/MS product ion spectrum of the $[M + H]^+$ ion. (**b**) CID-MS/MS product ion spectrum of the $[M + 2H]^{2+}$ ion. (**c**) CID MS^3 product ion spectrum of the $[M + H - CH_2CHCONH_2]^+$ neutral loss product ion from (**a**). (**d**) CID MS^4 product ion spectrum of the $[M + H - H_2O]^+$ neutral loss product ion from (**c**). Key: open triangle: $-H_2NCOCH_2CH_2SOH$; dagger: $-(CH_2CHCONH_2+H_2O)$; open circle: $-H_2O$.

$CH_2CH_2CONH_2$). The CIR values calculated from these spectra, as well as those calculated from dissociation of the singly and multiply protonated S-amidoethyl cysteine sulfoxide-containing peptides GAILCGAILR [C(S-ae)(ox)R] and VTMGHFCNFGK [M(ox)C(S-ae)(ox)K] that demonstrate the proton mobility dependence to these losses, are shown in Table 1.

CID-MS/MS of the uniformly deuterium exchanged C(S-ae)(ox)K peptide again confirmed that the loss of $H_2NCOCH_2CH_2SOH$ (XSOH) from the singly and doubly protonated precursor ions occurred via the *cis*-1,2 elimination reaction mechanism shown in pathway A of Scheme **1** (data not shown). H/D exchange experiments also confirmed that the neutral loss of $CH_2CHCONH_2$ (CH_2CHX', where $X' = CONH_2$) from these peptide ions occurred via a charge-remote *cis*-1,2 elimination reaction to yield the cysteine sulfenic acid-containing product ion **(2)**, as shown in pathway B of Scheme **1**. This is consistent with the mechanism recently proposed by Chowdhury et al. for the neutral loss of 4-vinylpyridine from S-pyridylethyl cysteine sulfoxide-containing peptides [8].

To obtain further insights into the relative abundances of the product ions formed via the side-chain losses of XSOH and CH_2CHX' from these peptides, a series of molecular orbital calculations were performed to determine the transition-state barriers associated with each reaction pathway, using the simple neutral model systems $CH_3CONHCH[CH_2S(O)CH_3]CONHCH_3$ and $H_2NCOCH_2CH_2S(O)CH_3$. Potential transition-state structures for each fragmentation pathway were initially examined at the PM3 semi empirical level of theory, followed by re-optimization of low-energy conformers at the B3LYP/6-31 + G(d,p) density functional level of theory. Vibrational frequency analysis was performed to confirm the nature of the optimized stationary point structure. Then, intrinsic reaction coordinate searches were performed, followed by geometry optimization at the same level of theory to locate the appropriate precursor and product ion structures associated with both transition states. The structures obtained from these calculations are shown in Figure 5. Structure [TS1] in Figure 5a shows the predicted low-energy transition-state structure found for the loss of CH_3SOH (equivalent to the loss of XSOH from the S-alkyl cysteine sulfoxide-containing peptides) from the model system $CH_3CONHCH[CH_2S(O)CH_3]CONHCH_3$ via a 5-membered *cis*-1,2 elimination pathway. IRC calculations, followed by geometry optimizations, were performed to locate the precursor ion [B] and the intermediate product ion [C] associated with this reaction coordinate. A further lower energy precursor

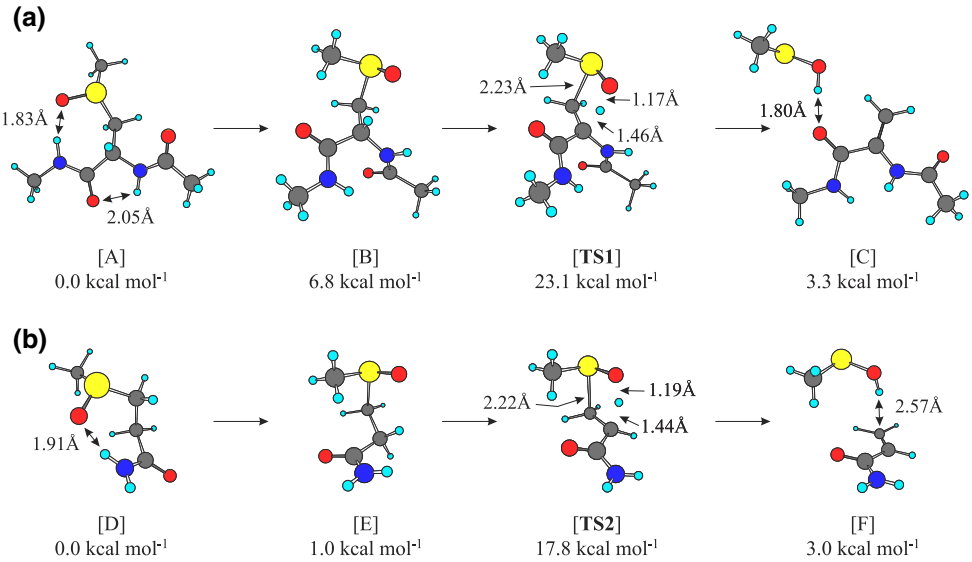

Figure 5. Optimized precursor, transition-state, and product ion structures (at the B3LYP/6-31 + G(d,p) + ZPVE level of theory) for (**a**) the loss of CH_3SOH from the neutral model system $CH_3CONHCH[CH_2S(O)CH_3]CONHCH_3$ (equivalent to the loss of XSOH from the S-alkyl cysteine sulfoxide-containing peptides) and (**b**) the loss of $CH_2CHCONH_2$ from the neutral model system $H_2NCOCH_2CH_2S(O)CH_3$ (equivalent to the loss of CH_2CHX' from the S-amidoethyl cysteine sulfoxide-containing peptides), via 5-membered *cis*-1,2 elimination pathways.

ion [A] was also located. The relative energy of the transition-state (+23.1 kcal mol^{-1}) was then calculated with respect to the energy of this precursor ion. Structure° [TS2]° in° Figure° 5b° represents° the° low-energy transition-state structure found for the neutral loss of $CH_2CHCONH_2$ (equivalent to the loss of CH_2CHX' from the S-amidoethyl cysteine sulfoxide-containing peptides) from the model system $H_2NCOCH_2CH_2S(O)CH_3$. After IRC calculations were performed, the associated precursor ion [E], the intermediate product ion [F], and a lower energy precursor ion [D] were located. The energy of the transition-state [TS2] with respect to that of the low-energy precursor ion was found to be +17.8 kcal mol^{-1}. The total energies, zero point vibrational energies (ZPVE) and relative energies obtained for all the optimized transition°structures°are°given°in°Table°3.°The°similar°predicted activation barriers for the two fragmentation reactions (i.e., −XSOH and $-CH_2CHX'$) are therefore consistent with the experimentally observed product ion abundances.

MS^3 dissociation of the neutral loss $[M + H - CH_2CHCONH_2]^+$° product°ion°from°Figure°4a°resulted in the exclusive loss of H_2O°(Figure°4c).°As°shown°in Scheme **3**, the neutral loss of H_2O may potentially occur via a charge-remote *cis*-1,2 elimination reaction (Scheme **3**, pathway A) to yield an amino thiopropanoic acid-containing product ion **(10)**. Alternatively, following intramolecular proton transfer from the peptide backbone to yield the protonated sulfenic acid intermediate **(11)**, the loss of H_2O could also potentially occur via a charge-directed E2 elimination reaction to yield **(12)** (Scheme **3**, pathway B), or via S_N2 neighboring group participation reactions involving the N- or C-terminal amide carbonyl groups adjacent to the side chain to yield a cyclic five-membered 1,2 oxathiolane product **(13)** (Scheme **3**, pathway C) or a six-membered 1,3,5 oxathiazine product (structure not shown), respectively. Hydrogen/deuterium exchange can readily be used to differentiate between the charge-remote and charge-directed fragmentation pathways proposed in

Table 3. Total energies (E_{total}), zero point vibrational energies (ZPVE) and relative energies (E_{rel}) computed for the precursor ions, transition states and product ion structures associated with each reaction pathway at the B3LYP/6-31 + G (d,p) level of theory

Structure	E_{total} (Hartree)	ZPVE (kcal mol^{-1})	E_{rel} (kcal mol^{-1})[a]
A	−1008.5887922	137.44180	0.0
B	−1008.5777340	137.34926	+6.8[b]
TS1	−1008.5459784	133.67822	+23.1[b]
C	−1008.5807054	135.69649	+3.3[b]
D	−761.2438197	85.48194	0.0
E	−761.2414516	85.01374	+1.06[c]
TS2	−761.2090719	81.44402	+17.8[c]
F	−761.2348465	82.84947	+3.0[c]
G	−839.6268943	111.59516	0.0
TS3	−839.5874485	107.78148	+20.9[d]
H	−839.6238461	109.49210	−0.2[d]
I	−840.0063802	120.51150	0.0
TS4	−839.9849623	117.08063	+10.0[e]
J	−840.0105422	118.44960	−4.7[e]

[a] E_{rel} = total energy + (ZPVE).
[b] Energy relative to Structure A.
[c] Energy relative to Structure D.
[d] Energy relative to Structure G.
[e] Energy relative to Structure I.

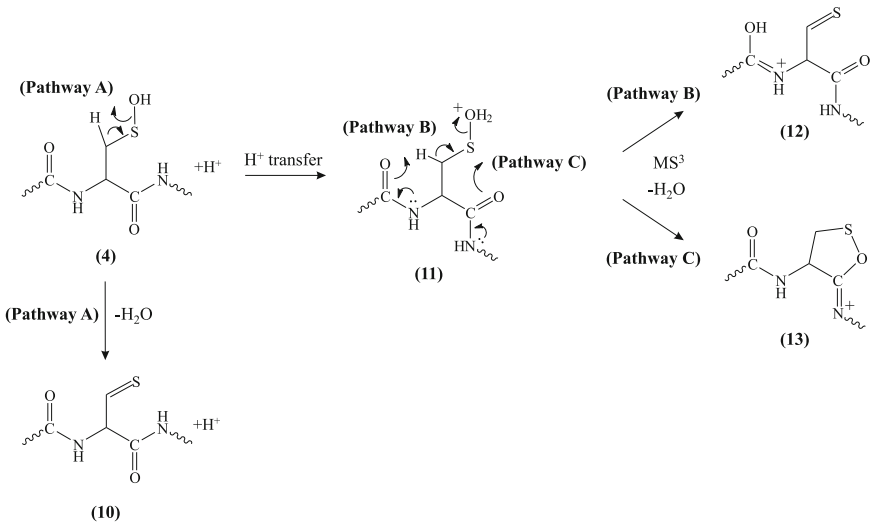

Scheme 3. Proposed mechanisms for the loss of H_2O from cysteine sulfenic acid-containing peptide ions.

Scheme **3**, which would result in the loss of H_2O and HOD, respectively. MS^3 dissociation of the $[M + D - CH_2CHCOND_2]^+$ product ion formed by dissociation of the uniformly deuterated $[M + D]^+$ precursor ion of the C(S-ae)(ox)K peptide resulted primarily in the neutral loss of D_2O (100% relative abundance), with only minor loss of HOD observed (approximately 10% relative abundance) (data not shown). This suggested that the hydroxyl hydrogen in the sulfenic acid side chain [Structure **(4)**] of the $[M + D - CH_2CHCOND_2]^+$ MS/MS product ion underwent exchange ("scrambling") with a deuterium on the peptide backbone before its dissociation by MS^3. Under these conditions, the charge-remote mechanism would primarily result in the neutral loss of HOD, while the charge-directed mechanisms would primarily result in the loss of D_2O. Therefore, we propose that the loss of H_2O from the $[M + H - CH_2CHCONH_2]^+$ ion occurs via a charge-directed process. The MS^4 spectrum obtained by dissociation of the $[M + H - CH_2CHCONH_2 - H_2O]^+$ product ion is shown in Figure 4d. Observation of the b_4, b_5, and y_6 ions in this spectrum, corresponding to cleavage of the amide bonds adjacent to the site of the cysteine side chain, suggests that the E2 elimination reaction had occurred. However, based on our recent study on the mechanisms responsible for the side-chain fragmentation reactions of methionine fixed charge sulfonium ion-containing peptides, where formation of a mixture of cyclic five- and six-membered product ions were found to be favored [19], the S_N2 neighboring group participation reactions cannot be ruled out.

In contrast to the data shown in Figure 4a, b, and Table 1, where the product ions formed via the losses of $H_2NCOCH_2CH_2SOH$ and $CH_2CHCONH_2$ (and/or $CH_2CHCONH_2+H_2O$) from the S-amidoethyl cysteine sulfoxide-containing peptides were observed at similar abundances for all the precursor ion charge states examined (i.e., independently of the proton mobility of the peptide ions), the product ion abundances of the side-chain losses from S-pyridylethyl

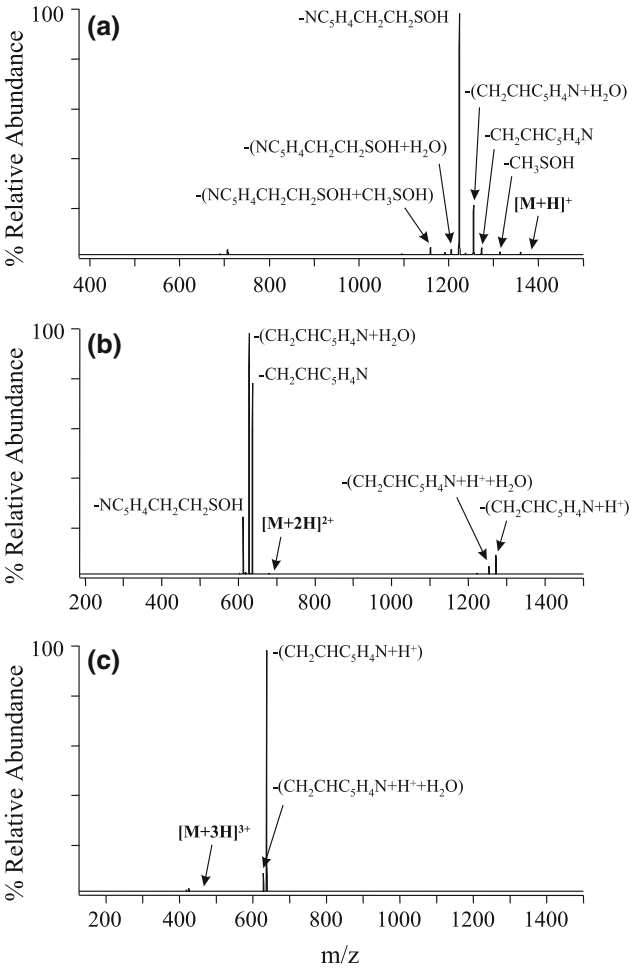

Figure 6. CID-MS/MS product ion spectra of the methionine sulfoxide- and S-pyridylethyl cysteine sulfoxide-containing peptide VTMGHFCNFGK [M(ox)C(S-pe)(ox)K]. (**a**) $[M + H]^+$ ion. (**b**) $[M + 2H]^{2+}$ ion. (**c**) $[M + 3H]^{3+}$ ion.

cysteine sulfoxide-containing peptides were observed to vary significantly depending on the proton mobility of the precursor ion. For example, Figure 6 shows the product ion spectra obtained by CID-MS/MS of the singly, doubly, and triply protonated precursor ions of the S-pyridylethyl cysteine sulfoxide-containing peptide VTMGHFCNFGK [M(ox)C(S-pe)(ox)K] (where pe = $CH_2CH_2C_5H_4N$) (Figure 6a, b, and c, respectively). The CIR values calculated for the loss of pyridylethyl sulfenic acid (−XSOH, 155 Da, where X = $CH_2CH_2C_5H_4N$) and vinylpyridine (−CH_2CHX', 105 Da, where X′ = C_5H_4N) from these ions, as well as those from the singly and doubly protonated S-pyridylethyl cysteine sulfoxide-containing peptides GAILCGAILK [C(S-pe)(ox)K] and GAILCGAILR [C(S-pe)(ox)R] are shown in Table 1. Note that the CIR values shown in Table 1 for the loss of CH_2CHX' also take into account the abundance of product ions formed via the combined losses of $CH_2CHC_5H_4N$ and H_2O ($CH_2CHX'+H_2O$, 123Da). It can be seen from Figure 6a that CID-MS/MS of the singly protonated precursor ion of M(ox)C(S-pe)(ox)K resulted primarily in the loss of $NC_5H_4CH_2CH_2SOH$ (XSOH), with the losses of $CH_2CHC_5H_4N$ (CH_2CHX') or $CH_2CHC_5H_4N$ + H_2O ($CH_2CHX'+H_2O$) observed at somewhat lower abundances. In contrast, the losses of $CH_2CHC_5H_4N$ (CH_2CHX') and $CH_2CHC_5H_4N$ + H_2O ($CH_2CHX'+H_2O$) from the doubly and triply protonated precursors (Figure 6b and c, respectively), were observed as the most abundant products. Furthermore, the observation of these losses as charged (protonated) species was observed to increase with increasing charge state (proton mobility). Similar trends were also observed from dissociation of the C(S-pe)(ox)K and C(S-pe)(ox)R peptide ions (Table 1).

The differences in fragmentation behavior observed between the S-pyridylethyl and S-amidoethyl cysteine sulfoxide-containing peptides can be rationalized by taking into consideration the expected sites of protonation in the singly and multiply protonated precursor ions of each of the peptides, and the effect of the site of protonation on the transition-state barriers for the loss of CH_2CHX' via the charge-remote *cis*-1,2 elimination pathway. The proton affinity of an appropriate model for the S-pyridylethyl cysteine sulfoxide side chain is 4-ethylpyridine (227.3 kcal mol^{-1}) [20]. Although this is lower than the proton affinities of arginine (251.2 kcal mol^{-1}) and lysine (238 kcal mol^{-1}), it is significantly higher than that of appropriate models for the S-amidoethyl cysteine sulfoxide side chain, i.e., propi-

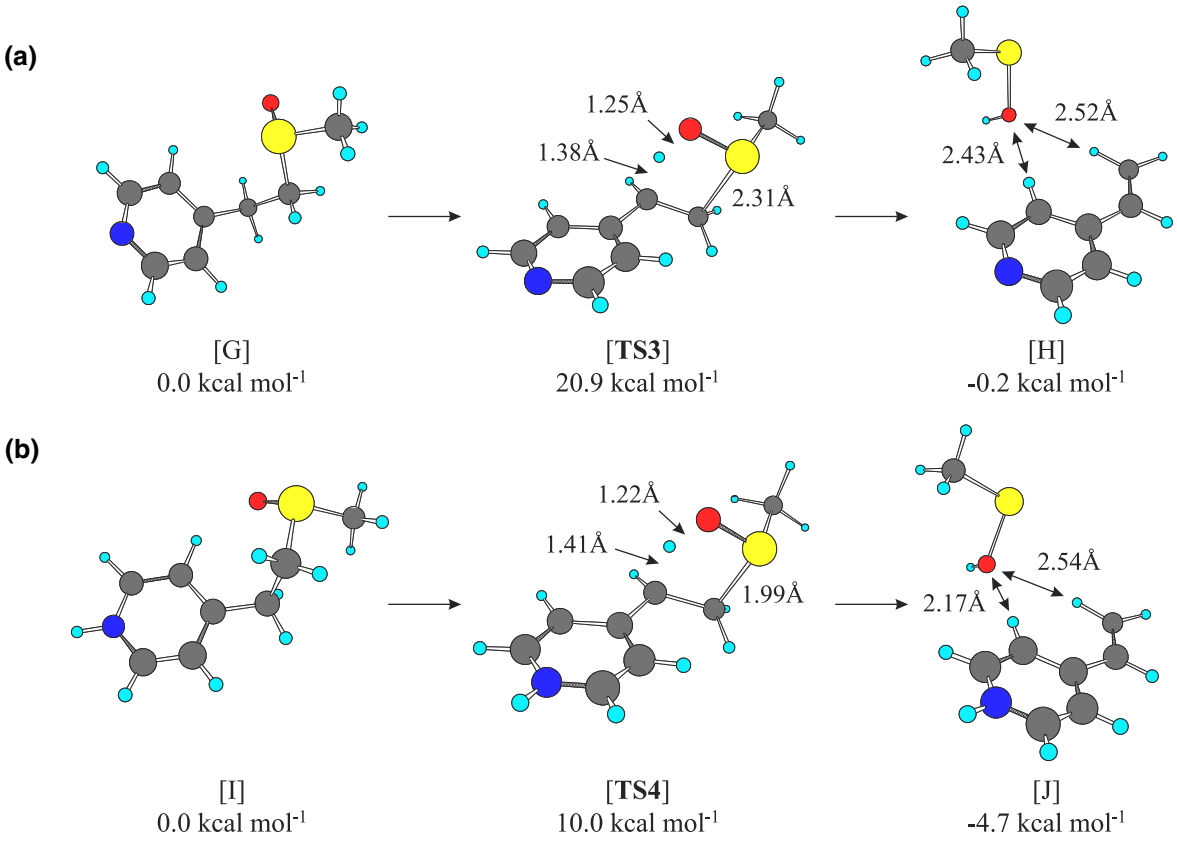

Figure 7. Optimized precursor, transition-state and product ion structures (at the B3LYP/6-31 + G(d,p) + ZPVE level of theory) for (**a**) the loss of $CH_2CHC_5H_4N$ from the neutral model system $NC_5H_4CH_2CH_2S(O)CH_3$ and (**b**) the loss of $CH_2CHC_5H_4NH^+$ from the protonated model system $HNC_5H_4CH_2CH_2S(O)CH_3^+$ (equivalent to the loss of CH_2CHX' from the S-pyridylethyl cysteine sulfoxide-containing peptides).

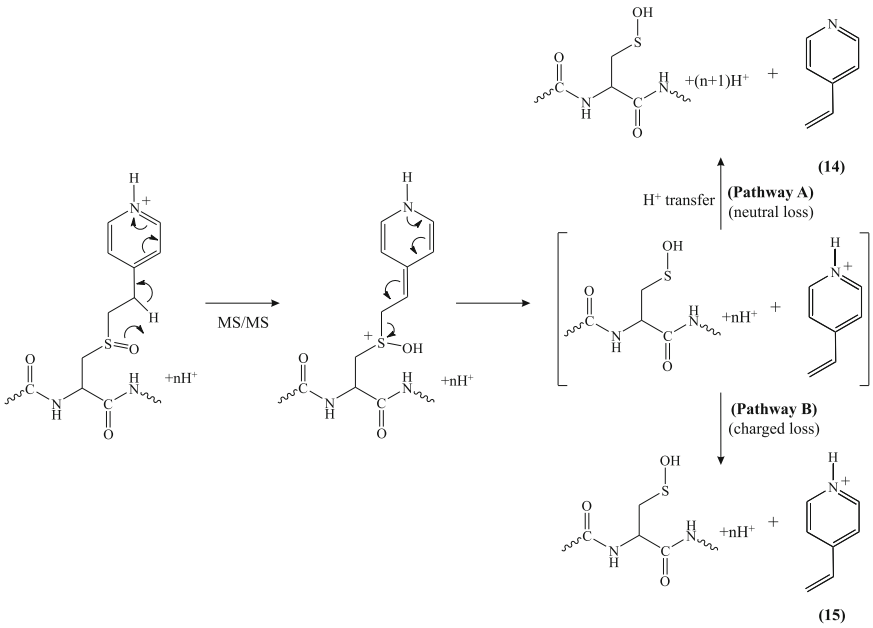

Scheme 4. Proposed mechanism for the loss of vinylpyridine from the protonated side chain of S-pyridylethyl (S-pe) cysteine sulfoxide-containing peptide ions.

onamide (209.4 kcal mol^{-1}) and the amide backbone (i.e., N-methylacetamide (212.4 kcal mol^{-1}) [20]. Therefore, the site of protonation for all the singly charged precursor ions examined here is expected to be at either the terminal lysine or arginine residues of the peptide sequence. In contrast, while the addition of a second ionizing proton would be expected to result in protonation along the amide backbone for the S-amidoethyl cysteine sulfoxide-containing peptides, thereby allowing backbone fragmentation processes to be observed (for example, see Figure 4b), a second ionizing proton added to the S-pyridylethyl cysteine sulfoxide-containing peptides would be expected to localize on the side-chain pyridylethyl moiety. The effect of this localized proton on the predicted barriers for loss of the side chain CH_2CHX' is shown in Figure 7. Similar to that shown in Figure 5b for the neutral loss of $CH_2CHCONH_2$, the barrier for this loss from the model system $NC_5H_4CH_2CH_2S(O)CH_3$ (equivalent to the loss of CH_2CHX' from the S-pyridylethyl cysteine sulfoxide-containing peptides) was predicted to be 20.9 kcal mol^{-1} (Structure [TS3] in Figure 7a). In contrast, protonation of the pyridylethyl side chain resulted in a predicted transition-state activation barrier of only 10.0 kcal mol^{-1} (Structure [TS4] in Figure 7b), resulting in the loss of $CH_2CHC_5H_4NH^+$. These data are therefore entirely consistent with the experimentally observed product ion abundances shown in Figure 6 and in Table 1.

Loss of CH_2CHX' from the side chain of the doubly and triply protonated precursor ions of the M(ox)C(S-pe)(ox)K peptide (Figure 6b and c) as predominantly a neutral versus protonated species, respectively, can be readily rationalized by the expected differences in proton affinity between the singly and doubly protonated peptide product ions and the neutral 4-vinylpyridine side-chain cleavage product (i.e., the order of proton affinities is expected to be $[M + H - CH_2CHC_5H_4N]^+ > CH_2CHC_5H_4N > [M + 2H - CH_2CHC_5H_4N]^{2+}$). Thus, for dissociation of the doubly protonated precursor ion, the proton affinity of the peptide product ion is higher than that of $CH_2CHC_5H_4N$, such that proton transfer within the initially formed ion–ion complex results in loss of the side chain 4-vinylpyridine product as a neutral species (Scheme **4**, pathway A), while for dissociation of the triply protonated precursor ion, the proton affinity of the peptide product ion is lower than that of $CH_2CHC_5H_4N$, such that loss of the 4-vinylpyridine product is observed as the protonated species (Scheme **4**, pathway B).

Conclusions

The results presented here confirm that the loss of XSOH from the side chains of oxidized S-alkyl cysteine-containing peptides formed by reaction with iodomethane, iodoacetamide, iodoacetic acid, acrylamide, and 4-vinylpyridine occurs via a charge-remote five-centered *cis*-1,2 elimination reaction to yield a dehydroalanine-containing product ion. The mechanisms and proton mobility dependence to the losses of CO_2, $CO_2 + H_2O$, and $CO_2 + CH_2O$ from S-carboxymethyl cysteine sulfoxide-containing peptides, the loss of $CH_2CHC_5H_4N$ from S-amidoethyl cysteine sulfoxide-containing peptides, and the losses of $CH_2CHC_5H_4N$ and $CH_2CHC_5H_4NH^+$ from S-pyridylethyl cysteine sulfoxide-containing peptides following CID-MS/MS have also been examined. Clearly, both the nature of the S-alkyl substituent and the proton mobility of the peptide precursor ion have a significant

influence on the appearance of the product ion spectra obtained via the gas-phase dissociation of protonated S-alkyl cysteine sulfoxide-containing peptide ions. It is expected that incorporation of the non-sequence ion fragmentation behaviors observed here into the suite of "rules" employed by automated database search algorithms for protein identification should enable the development of more comprehensive tools for the identification and characterization of modified proteins.

Acknowledgments

Support for this work was provided by a National Science Foundation CAREER award to GER (grant no: CHE 0547940). JMF acknowledges the award of a U.S. Department of Homeland Security Fellowship, which is administered by the Oak Ridge Institute for Science and Education (ORISE) through an interagency agreement with the U.S. Department of Energy (DOE).

References

1. Sechi, S.; Chait, B. T. Modification of Cysteine Residues by Alkylation. A Tool in Peptide Mapping and Protein Identification. *Anal. Chem.* **1998,** *70*, 5150–5158.
2. Simpson, R. J.; Connelly, L. M.; Eddes, J. S.; Pereira, J. J.; Moritz, R. L.; Reid, G. E. Proteomic Analysis of the Human Colon Carcinoma Cell Line (LIM 1215): Development of a Membrane Protein Database. *Electrophoresis* **2000,** *21*, 1707–1732.
3. Moritz, R. L.; Eddes, J. S.; Reid, G. E.; Simpson, R. J. S-Pyridylethylation of Intact Polyacrylamide Gels and in-Situ Digestion of Electrophoretically-separated Proteins: A Rapid Mass Spectrometric Method for Identifying Cysteine-Containing Peptides. *Electrophoresis* **1996,** *17*, 907–917.
4. Shevchenko, A.; Wilm, M.; Vorm, O.; Mann, M. Mass Spectrometric Sequencing of Proteins from Silver-Stained Polyacrylamide Gels. *Anal. Chem.* **1996,** *68*, 850–858.
5. Swiderek, K. M.; Davis, M. T.; Lee, T. D. The Identification of Peptide Modifications Derived from Gel-Separated Proteins Using Electrospray Triple Quadrupole and Ion Trap Analyses. *Electrophoresis* **1998,** *19*, 989–997.
6. Steen, H.; Mann, M. Similarity Between Condensed Phase and Gas Phase Chemistry: Fragmentation of Peptides Containing Oxidized Cysteine Residues and its Implications for Proteomics. *J. Am. Soc. Mass Spectrom.* **2001,** *12*, 228–232.
7. Yagüe, J.; Núñez, A.; Boix, M.; Esteller, M.; Alfonso, P.; Casal, J. I. Oxidation of Carboxyamidomethyl Cysteine may add Complexity to Protein Identification. *Proteomics* **2005,** *5*, 2761–2768.
8. Chowdhury, S. M.; Munske, G. R.; Ronald, R. C.; Bruce, J. E. Evaluation of Low Energy CID and ECD Fragmentation Behavior of Mono-oxidized Thio-Ether Bonds in Peptides. *J. Am. Soc. Mass Spectrom.* **2007,** *18*, 493–501.
9. Hunt, D. F.; Yates, J. R. III; Shabanowitz, J.; Winston, S.; Hauer, C. R. Protein Sequencing by Tandem Mass Spectrometry. *Proc. Natl. Acad. Sci. U.S.A.* **1986,** *83*, 6233–6237.
10. Eng, J. K.; McCormack, A. L.; Yates, J. R. III. An Approach to Correlate Tandem Mass Spectral Data of Peptides with Amino Acid Sequences in a Protein Database. *J. Am. Soc. Mass Spectrom.* **1994,** *5*, 976–989.
11. Perkins, D. N.; Pappin, D. J. C.; Creasy, D. M.; Cottrell, J. S. Probability-Based Protein Identification by Searching Sequence Databases using Mass Spectrometry Data. *Electrophoresis* **1999,** *20*, 3551–3567.
12. Gruhler, A.; Olsen, J. V.; Mohammed, S.; Mortensen, P.; Faergeman, N. J.; Mann, M.; Jensen, O. N. Quantitative Phosphoproteomics Applied to the Yeast Pheromone Signaling Pathway. *Mol. Cell. Proteomics.* **2005,** *4*, 310–327.
13. Wolschin, F.; Lehmann, U.; Glinski, M.; Weckwerth, W. An Integrated Strategy for Identification and Relative Quantification of Site-Specific Protein Phosphorylation using Liquid Chromatography Coupled to MS^2/MS^3. *Rapid Commun. Mass Spectrom.* **2005,** *19*, 3626–3632.
14. Reid, G. E.; Roberts, K. D.; Kapp, E. A.; Simpson, R. J. Statistical and Mechanistic Approaches to Understanding the Gas-Phase Fragmentation Behavior of Methionine Sulfoxide-Containing Peptides. *J. Prot. Res.* **2004,** *3*, 751–759.
15. Kapp, E. A.; Schütz, F.; Reid, G. E.; Eddes, J. S.; Moritz, R. L.; O'Hair, R.A. J.; Speed, T. P.; Simpson, R. J. Mining a Tandem Mass Spectrometry Database to Determine the Trends and Global Factors Influencing Peptide Fragmentation. *Anal. Chem.* **2003,** *75*, 6251–6264.
16. Frisch, M. J.; Trucks, G. W.; Schlegel, H. B.; Scuseria, G. E.; Robb, M. A.; Cheeseman, J. R.; Zakrzewski, V. G.; Montgomery, J. A.; Stratman, R. E.; Burant, J. C.; Dapprich, S.; Millam, J. M.; Daniels, A. D.; Kudin, K. N.; Strain, M. C.; Farkas, O.; Tomasi, J.; Barone, V.; Cossi, M.; Cammi, R.; Mennucci, B.; Pomelli, C.; Adamo, C.; Clifford, S.; Ochterski, J.; Petersson, G. A.; Ayala, P. Y.; Cui, Q.; Morokuma, K.; Malick, D. K.; Rabuck, A. D.; Raghavachari, K.; Foresman, J. B.; Cioslowski, J.; Ortiz, J. V.; Baboul, A. G.; Stefanov, B. B.; Liu, G.; Liashenko, A.; Piskorz, P.; Komaromi, I.; Gomperts, R.; Martin, R. L.; Fox, D. J.; Keith, T.; Al-Laham, M. A.; Peng, C. Y.; Nanayakkara, A.; Gonzalez, C.; Challacombe, M.; Gill, P. M. W.; Johnson, B.; Chen, W.; Wong, M. W.; Andres, J. L.; Gonzalez, C.; Head-Gordon, M.; Replogle, E. S.; Pople, J. A. *Gaussian 98, Revision A.7*; 1998, Gaussian Inc.: Pittsburgh PA.
17. Yang, F.; Stenoien, D. L.; Strittmatter, E. F.; Wang, J.; Ding, L.; Lipton, M. S.; Monroe, M. E.; Nicora, C. D.; Gristenko, M. A.; Tang, K.; Fang, R.; Adkins, J. N.; Camp, D. G.; Chen, D. J.; Smith, R. D. Phosphoproteome Profiling of Human Skin Fibroblast Cells in Response to Low- and High-Dose Irradiation. *J. Prot. Res.* **2006,** *5*, 1252–1260.
18. Beausoleil, S. A.; Villén, J.; Gerber, S. A.; Rush, J.; Gygi, S. P. A Probability-Based Approach for High-Throughput Protein Phosphorylation Analysis and Site Localization. *Nat. Biotechnol.* **2006,** *24*, 1285–1292.
19. Amungama, M.; Roberts, K. D.; Reid, G. E. Mechanisms for the Selective Gas-Phase Fragmentation Reactions of Methionine Side Chain Fixed Charge Sulfonium Ion-Containing Peptides. *J. Am. Soc. Mass Spectrom.* **2006,** *17*, 1631–1642.
20. Hunter, E. P.; Lias, S. G. Evaluated Gas Phase Basicities and Proton Affinities of Molecules: An Update. *J. Phys. Chem. Ref. Data* **1998,** *27*, 413–656.